# Structure, Stability, and Electronic and Magnetic Properties of VGen (n=1-19) Clusters

C. Siouani, S. Mahtout, S. Safer, Franck Rabilloud

# Structure, Stability and Electronic and Magnetic Properties of $VGe_n$ (n=1-19) Clusters

C. SIOUANI[a], S. MAHTOUT[a*], S. SAFER[a] and F. RABILLOUD[b*]
[a] *Laboratoire de Physique Théorique, Faculté des Sciences Exactes, Université de Bejaia, 06000 Bejaia, Algérie.*
[b] *Univ Lyon, Université Claude Bernard Lyon 1, CNRS, Institut Lumière Matière, F-69622, Villeurbanne, France*
[*] *Corresponding authors: mahtout_sofiane@yahoo.fr, franck.rabilloud@univ-lyon1.fr*

## Abstract

We systematically study the equilibrium geometries, electronic and magnetic properties of $Ge_{n+1}$ and $VGe_n$ (n = 1–19) clusters using the density functional theory approach (DFT) within the generalized gradient approximation (GGA). Endohedral structures in which the vanadium atom is encapsulated inside a $Ge_n$ cage are predicted to be favored for $n \geq 10$. The dopant V atom in the $Ge_n$ clusters has not an immediate effect on the stability of small germanium clusters (n<6) but it largely contributes to strengthen the stability for $n \geq 7$. Our study enhances the large stability of the $VGe_{14}$ cluster which presents an $O_h$ symmetry cage-like geometry and a peculiar electronic structure in which the valence electrons of V and Ge atoms are delocalized and exhibit a shell structure associated to the quasi-spherical geometry. Consequently, this cluster is proposed to be a good candidate to be used as the building blocks for developing new materials. The cluster size dependence of the stability, the vertical ionization potentials and electron affinities of $Ge_{n+1}$ and $VGe_n$ are presented. Magnetic properties and the partial density of states of the most stable $VGe_n$ clusters are also discussed.

## 1. Introduction

For several decades, the properties of small, intermediate and large sized clusters have been intensively investigated because of their potential applications in nanotechnologies. It is well know that most of physical and chemical properties of small and intermediate sized clusters are greatly determined by the size, composition and shape. In particular, the properties may change dramatically with the addition or substitution of one or few atoms in the cluster.

Semiconductor clusters doped with transition metal (TM) atoms are expected to yield interesting magnetic, electronic and optical properties for eventual applications in materials science, microelectronics, biological and medical area. The doping is used to control electronic and magnetic properties, or to stabilize peculiar structures. In particular, the experimental evidences of the formation of stable Si cages in which Si atoms encage a metal atom, as suggested earlier by theoretical calculations, has opened new perspectives to build cluster-assembled materials[1-5]. Germanium is also an important semiconductor material.

Extensive experimental and theoretical investigations on the pure and metal-doped Ge clusters were reported in the last decade[6-44]. An experimental atomic scale observation of the dynamical behaviour of small germanium clusters combined with ab initio calculations have suggested that seven-membered rings, trigonal prisms and some smaller subunits are possible building blocks that stabilize the structure germanium cage clusters[39]. From the theoretical point of view, several calculations have suggested that a $Ge_n$ cage can be stabilized by encapsulating a guest metal atom inside the cage, as it was previously shown in the case of $Si_n$ cages. However the growth patterns of the TM-doped germanium clusters are dependent on the metal atom. For examples, density functional theory (DFT) calculations have shown that the doping Cu atom enhances the stability of the $Ge_n$ cluster from n=10 and the electron charge transfers from the Cu atom to the neighbooring Ge atoms[11,18]. Using First-principles calculations, Jing et al.[15] observed that the doping by Co atom enhances the stability of germanium cluster host without quenching the total magnetic moment. More recently, in a photoelectron spectroscopy study combined with DFT calculations, Deng et al.[16] found that the magnetic moment of the anionic and neutral $CoGe_n^{(-)}$ clusters decreases to the lowest values for sizes n = 10 and 11. For Ni doped germanium clusters, Ni atom was found to be encapsulated inside a germanium cage for clusters containing more than 8 atoms, while the large and peculiar stability of $NiGe_{10}$ were explained by the electron counting rule as the cluster size corresponds to 20 valence electrons[22,28]. Wang and Han[23] also investigated the doping with tungsten and demonstrated that $WGe_{12}$, $WGe_{14}$, $WGe_{16}$ structures enhance stabilities over their neighboring clusters while the electron charge transfer always is done from the germanium framework to the W atom. In their ab initio investigation on the properties of thorium encapsulated germanium cages clusters with the size of 16, 18 and 20 atoms, Singh et al.[21] have reported that the doping atom is located at the center of the cage and the binding energies of doped clusters are enhanced in comparison to the pure germanium clusters with the same sizes. According to the DFT study by Kapila et al.[34] the growth behavior of $CrGe_n$ for $n \leq 13$ shows preference of Cr atom to stabilize at the exohedral position but the doping with Cr atom does not enhance the cluster stability, while Hou et al.[40] have found that small $CrGe_n$ clusters prefer structures with high-spin ground state and large magnetic moments. More recently, Mahtout et al.[44] show that the encapsulation of Cr atoms within $Ge_n$ clusters leads to stable $CrGe_n$ (n=15-29) clusters and the electronic and magnetic properties depend on the structure and the position of Cr atom in the clusters. The $FeGe_n$ clusters were investigated by Zhao and Wang[42], while anionic $AuGe_n^-$ species were considered by Li et al.[36]. The properties of bimetallic $Mo_2$ doped germanium clusters in the size range of 9 to 15 atoms were also investigated at DFT level[24]. It was shown that the most stable structures are obtained when one Mo atom is inside of the $Ge_n$ cage and the second is located at the surface for $n \leq 13$ atoms. But $Mo_2$ dimer was completely encapsulated into the germanium cage when the cluster size is larger. Considering Mn doped germanium clusters, Zhao and Wang[38] found that the doping by one Mn atom contributes to enhance the stability of the germanium cage clusters while the charge transfers were done from Mn to the neighboring Ge atoms. However they found that the magnetic moment of the Mn atom does not quench in all Ge cage clusters. Kapila et al.[36] investigated the effects of doping with several transition metal atom (Mn, Co and Ni) on the properties of Ge cage clusters. They found that the total magnetic moment is localized at the doping atom and neighboring Ge atoms and the Ni doped $Ge_n$ clusters are the most stable compared to other Co and Mn doped $Ge_n$ clusters. Very recently, an inherent tendency of formation of an endohedral cage were reported for multicharged ruthenium-doped Ge clusters[9].

The reading of the previous works shows that geometric, electronic and magnetic properties of transition metal doped germanium clusters are significantly different from those of pure $Ge_n$ ones, and change dramatically with their size and the nature of doping metal

atoms. To our knowledge, the doping of germanium clusters with vanadium atoms has been considered in two previous works[7,8]. First, studying the relative stability of Sc, Ti, and V encapsulating $Ge_n$ (n=14-20) clusters in both neutral and charged states, it was explored how far any enhanced stability can be explained by the formation of a closed shell free-electron gas inside the Ge cages, and if an electron-rich region spread uniformly around the metal atom can be unequivocally identified and visualized using the topological features of the molecular electrostatic potential[7]. The analysis was based on a naive electron counting, where each Ge atom is supposed to donate one electron to the free-electron gas while V atom gives 5 electrons. Therefore $VGe_{15}$ and $VGe_{16}^+$ are possible 20-electron clusters, and were predicted to have an enhanced stability. Recently, in a joint experimental and theoretical investigation, the photoelectron spectra of $VGe_n^-$ ($n \leq 12$) were measured and compared to DFT calculations on putative structures for both anionic and neutral species[8]. However, both studies focused on a restricted cluster size range, and there is a clear need to rationalize these studies to a wider size range in order to highlight a growth pattern, while performing a more extended search for the lowest isomer with new putative structures.

The present work aims to understand the influence of one vanadium atom on germanium clusters and to study the different properties of the $VGe_n$ clusters that will be compared to other metal doped germanium clusters. So, the geometric structures, relative stabilities, electronic and magnetic properties of small $VGe_n$ (n=1-19) clusters have been systematically investigated by using first principles calculations. The structures of low-lying energy isomers of each cluster size have been optimized and analysed, as well as the binding energy, HOMO-LUMO gaps, vertical ionization potential and vertical electron affinity. This paper is organized as followed: we describe in section 2 the computational method used in this work, while results and discussion on the clusters geometries, stabilities, electronic and magnetic properties of $VGe_n$ clusters, and also the peculiar case of $VGe_{14}$, are presented in Section 3. Finally, our main conclusions are given in Section 4.

## 2. Computational methodology

All calculations were performed using the spin polarized density functional theory implemented in the SIESTA package[45]. They were carried out using the generalized gradient approximation formulated by Perdew, Burke, and Ernzerhof[46] (PBE) to describe the exchange–correlation energy functional. The norm-conserving Troullier–Martins nonlocal pseudopotentials[47] were used together with a flexible basis set of localized Gaussian-type atomic orbitals. Then, core electrons were replaced by non-local, norm-conserving pseudopotentials factorized in the Kleinman–Bylander form[48]. We have used $3d^3$ $4s^2$ configuration for V and $4s^2$ $4p^2$ for Ge. The geometries have been optimized without any symmetry constraints and the optimization of electronic structure was obtained by solving the Kohn–Sham equations[49] self-consistently with a convergence criterion of $10^{-4}$a.u. on the energy and electron density. We have used the k=0 (Γ) point approximation for Brillouin zone sampling. We have used the double ζ (DZ) basis for Ge atoms and double ζ (DZP) bases with polarization function for V atom. In the optimization process, the volume of the system was kept constant and with a big supercell of 40 Å was used in order to avoid interaction between the neighboring clusters. Structural optimizations are performed using conjugate gradient algorithm and the convergence criterion on the Hellmann Feynman forces imposed that the residual forces were smaller than 0.04 eV/Å. Several spin multiplicity states were tested. The Mulliken population analyses were done in order to obtain the atomic charge and the unpaired spin population. The validity of current computational method has been tested on germanium dimer properties. The obtained results are summarized in Table 1 and compared to the available theoretical and experimental data. Our calculated bond length of 2.450 Å and

dissociation energy of 1.446 eV are consistent with the literature. They show the reliability of current computational scheme to describe small germanium clusters. For the dimer VGe, the electronic ground state is found to be a sextet with a bond distance of 2.526 Å and a binding energy of 1.198 eV. To the best of our knowledge, there is no available experimental or calculated value.

## 3. Results and discussion

### 3.1. Structural properties

It is well known that the number of isomers increases exponentially with increasing cluster size, making it challenging job to search for the most lowest-energy structure. In order to obtain the global minimum structures of $Ge_{n+1}$ and $VGe_n$ clusters, we have optimized a large number of possible isomeric structures. Lots of possible initial structures including one, two or three dimensional (3D) configurations have been considered for each size, amongst others some initial structures of $Ge_{n+1}$ and metal-doped $Ge_n$ clusters were taken from literature. Also, the putative structures of $VGe_n$ have been obtained by local relaxation after the substitution of one Ge atom by V atom in several isomers of the original pure $Ge_{n+1}$ cluster. The different initial positions of the V atom in the $Ge_{n+1}$ clusters lead to different $VGe_n$ isomers. Of course, the explicit treatment of the electronic structure constitutes a demanding computational task, and the search for the lowest isomer cannot include a global optimization procedure of the potential energy surface. So we cannot be sure that a more stable cluster than those found in our calculations does not exist. In this work we only show the best calculated structures for each cluster size. The stability of the structures was checked by calculating their harmonic vibrational frequencies. If any imaginary frequency was found, further relaxation was carried out until the true local minimum was obtained.

In the case of pure $Ge_{n+1}$ clusters, our calculations show a growth pattern in which the planar structures only appears in the very small clusters while the tridimensional structures dominate from n+1=5. Up to n+1=20, prolate-type structures compete with nearly spherical structures, and almost all atoms are located in surface. Many of the obtained best structures are in agreement with the previous theoretical studies of the literature. Our lowest-energy isomers are shown in Figure 1, while the energetic ordering of isomers are given Table 2. For each size, data for most stable isomer are reported in bold character. For clusters with n=2 and 3, the ground state structures adopt a planar form in agreement with previous works[11, 28, 30] by using different density functional calculations. Both linear and triangular structures are considered for the $Ge_3$. The triangular geometry with $D_{3h}$ symmetry and average bond length of 2.342 Å is found to be the most stable structure. The most stable isomer of the tetramer $Ge_4$ has $D_{2h}$ symmetry and an average bond length of 2.577 Å which are in good agreement with previous works[11,28,33]. The three dimensional geometries appears for n=4. The $Ge_5$ pentamer ground state is a triangular bipyramid structure with $D_{3h}$ symmetry and an average bond length of 2.548 Å. This result is consistent with the previous theoretical results[11,28,34]. For $Ge_6$, two isomers are found to be quasi-degenerate, the first one is a bicapped rectangular structure with $C_s$ symmetry and an average bond length of 2.744 Å, while the second one is a bicapped quadrilateral structure with $D_{4h}$ symmetry. The $C_s$-symmetry structure has been predicted to be the lowest-energy isomer in some previous works[28], while the $D_{4h}$ symmetry is preferred in other works[34]. In our calculation, the high-symmetry structure is found to lie 0.006 eV above the $C_s$ one, but it seems clear that the ordering may change with the functional or the basis set used. The lowest-energy $Ge_7$ cluster displays a pentagonal bipyramid structure of $D_{5h}$ symmetry and Ge-Ge bond at 2.747 Å which are in good agreement with the results of Wang

and Han[11] and Kapila et al.[34]. The most stable isomer for $Ge_8$ cluster presents a capped pentagonal bipyramid structure with $C_s$ symmetry, in agreement with previous works[11,34]. For $Ge_9$ cluster, a capped cube-like structure with $C_{4v}$ symmetry is found to be the most stable isomer. Its average bond length is calculated to be 2.663 Å. A similar result of $Ge_9$ is obtained by Bandyopadhyay and Sen[28]. In the case of $Ge_{10}$, the most stable structure is calculated to be a capped irregular pentagonal prism structure with $C_1$ symmetry and an average bond length of 2.748 Å (labeled $Ge_{10}$-c in Figure 1). A more regular structure with $D_{2h}$ symmetry (labeled $Ge_{10}$-a in Figure 1) is found to lie 0.06 eV above the previous one. The shape of $Ge_{11}$ is a caped pentagonal basis structure and with a $C_{2v}$ symmetry and an average bond length of 2.839 Å. For $Ge_{12}$ clusters, the most stable structure ($Ge_{12}$-f) is a compact near spherical structure with $C_{2v}$ symmetry, but a more prolate-like structure ($Ge_{12}$-a) is found to lie 0.04 eV above. From $Ge_{13}$ to $Ge_{16}$ clusters, a prolate structure with $C_1$ symmetry is always favored. The average bond lengths are 2.811, 2.725, 2.791 and 2.759 Å for n=13, 14, 15, 16 respectively. The best isomers of $Ge_{17}$ ($Ge_{17}$-a) has a near spherical shape with $C_s$ symmetry and an average bond length of 2.805 Å. In the case of the $Ge_{18}$ cluster, our calculations suggest that the prolate-like isomer $Ge_{18}$-b with $C_2$ symmetry and an average bond length of 2.732 Å is the most stable one. The lowest-energy isomer for $Ge_{19}$ has a prolate shape ($Ge_{19}$-a) and an average bond length of 2.769 Å whereas the most stable structure of $Ge_{20}$ ($Ge_{20}$-b) adopts a $C_1$ symmetry with a larger average bond length of 2.812 Å.

We now present our results concerning $VGe_n$ clusters. Optimized structures are showed in Figure 2, and energies are given in Table 3. Up to n=9, $VGe_n$ clusters adopt a somewhat similar structure than their corresponding $Ge_{n+1}$, with two exceptions, $VGe_3$ which prefers a compact tridimensional structure while $Ge_4$ is a rhombus and $VGe_8$ which significantly differs from the $C_{4v}$-symmetry structure of $Ge_9$. Interestingly, for n=10-16, the vanadium atom forms a core surrounded by all Ge atoms which in turn form an opened cage for n=10 and 11 and a fully closed cage for n=12-16 in which V is encapsulated. Then, for larger size, we see a competition between some prolate- and cage-like structures. The most stable structure of $VGe_{19}$ cluster (labelled $VGe_{19}$-c in figure 3) can be described as a cage-like structure $V@Ge_{11}$ anchored by three Ge atoms to the remainder of the cluster. This could mean that the cage $V@Ge_n$ may be used as the building blocks to make cluster-assembled materials. Clearly, the substitution of one Ge atom by a V atom leads to significant deformation for n>9. Similar conclusions can be done if we look at the deformation induced by introducing a V atom in a host $Ge_n$ cluster.

We now describe the structures of $VGe_n$ clusters in more details. The lowest-energy $VGe_2$ cluster displays a triangular structure of $C_{2v}$ symmetry. This ground-state structure has two equivalent V-Ge bonds 2.536 Å and one Ge-Ge bond 2.405 Å. The Ge-Ge distance is 0.063 Å larger than in the case of $Ge_3$ trimer and the V–Ge bond distance is 0.01 Å larger than in VGe dimer. For the $VGe_3$ tetramer, two low-lying structures are found as local minima. The first one presents a planar $C_{2v}$ symmetry and the second one is a triangular pyramid with $C_{3v}$ symmetry. This later is the lowest-energy isomer. Its calculated binding energy equals 2.350 eV/atom and is much smaller than that of the ground state of pure germanium tetramer $Ge_4$ (2.556 eV/atom). The most stable structure of $VGe_4$ cluster is a distorted rectangular pyramid with $C_s$ symmetry. The V-Ge and Ge-Ge bond lengths are 2.600 and 2.713 Å respectively. Its binding energy is 0.147 eV/atom and is smaller than that $Ge_5$. The lowest-energy structure of $VGe_5$ is a quasi-rectangular bipyramid with $C_{2v}$ symmetry and the V atom located at the convex site. The different V-Ge bond distances vary from 2.643 Å to 2.901 Å and the average Ge-Ge bond distance is found to be 2.704 Å. For $VGe_6$, two structures, with $C_{2v}$ and $C_{3v}$ point group symmetry respectively, compete for the lowest-energy isomer. In the latter, the $a_{V\text{-}Ge}$ bond lengths are much shorter (2.494 Å versus 2.746 Å). The lowest energy

isomer for $VGe_7$ cluster ($VGe_7$-b) can be described as a germanium atom capping a pentagonal bipyramid with the V atom at the vertex. This stable structure with $C_s$ symmetry is obtained by the substitution of a Ge atom by V in the ground state geometry $Ge_8$-b of pure cluster $Ge_8$. Its binding energy is only 0.002 eV/atom larger than the case of corresponding pure cluster. The global minimum structure of the $VGe_8$ cluster is the tricapped trigonal prism geometry ($VGe_8$-d) with the V atom at the surface (structure similar to that obtained in ref 8). The total spin magnetic moment is only 1 $\mu_B$. Its binding energy is 2.966 eV/atom and so 0.12 eV/atom higher than that of its corresponding pure isomer $Ge_9$-d. In $VGe_9$ cluster, the ground state geometry ($VGe_9$-e) can be described as a combination of two distorted hexagonal prism with V atom at the top of one of them. Let us note that the second isomer ($VGe_9$-f) found to lie 0.04 eV/atom above $VGe_9$-e will be used to build cage structures for $n \geq 10$. From n=10 our obtained clusters show an increasing tendency to encapsulate the vanadium at the center of the structure. In other words, the V-encapsulated germanium clusters become the dominant geometries. For $VGe_{10}$ cluster, the named $VGe_{10}$-c structure with V atom partially encapsulated in an opened $Ge_{10}$ cage with $C_{2v}$ symmetry is the ground state isomer. Its binding energy is 0.099 eV/atom larger than that of the corresponding pure cluster $Ge_{11}$-c. For $VGe_{11}$, the V atom tends to stabilize at the surface rather than at the central encapsulated position. Our lowest energy structure ($VGe_{11}$-a) is a distorted superposition of two rhombic structure with $C_{2v}$ symmetry and bond-lengths of 2.689 Å and 2.920 Å for Ge-Ge and V-Ge respectively. The lowest-energy structure ($VGe_{12}$-f) of the $VGe_{12}$ cluster is a perfect hexagonal prism geometry with V atom encapsulated at the center of the germanium cage with $D_{3d}$ symmetry. The second ($VGe_{12}$-d) and third ($VGe_{12}$-e) lowest isomers are also closed cage with $C_s$ and $D_{4h}$ symmetry. Endohedral structures have been already found for Mn-, Co-, Ni- Ti- doped $Ge_{12}$ [15,21,37,38]. For n=13, the ground-state ($VGe_{13}$-a) is a capped hexagonal prism structure with the V atom totally encapsulated at the center of the cage. The high $C_{6v}$ symmetry is found for this doublet spin state. Four V-encapsulated geometries have been found for $VGe_{14}$ cluster. The most stable one ($VGe_{14}$-a) presents the high $O_h$ symmetry with a large binding energy of 3.183 eV/atom. That structure has already been found as the lowest-energy isomer in the case of $WGe_{14}$ [23] and one of the stable structures but not in competition for the most stable isomer in $NiGe_{14}$ [28] or $CuGe_{14}$ [18]. For n=15, the optimized ground state structure is the endohedral structure $VGe_{15}$-c. It can be viewed as addition of one Ge atom at vertices of the isomer $VGe_{14}$-a. This geometry with $C_s$ symmetry is 0.127 eV/atom more stable than the corresponding most stable germanium clusters with the same size ($Ge_{17}$). It has the shortest Ge-Ge and largest V-Ge average bond lengths of 2.755 Å and 3.005 Å respectively. Kumar et al.[17] have also reported that adding one Ge atom to the bottom of the rhombi in a symmetrical hexagonal bi-capped structure TM-$Ge_{14}$ may leads to the ground state structure of TM-$Ge_{15}$ clusters. All of the ground state geometries for the bigger clusters ($n \geq 16$) in the present study show distorted structures. Particularly the endohedral structures become strongly deformed cages because a unique V atom cannot stabilize a perfect cage when the number of Ge atoms is too high. In the case of $VGe_{16}$, the irregular cage-like structure $VGe_{16}$-d is found to be the lowest isomer while the more regular $D_{2h}$ isomer (VGe-a) lie 0.68 eV above. For $VGe_{17}$, a prolate structure were found to be the ground state ($VGe_{17}$-a) while no cage-like isomer was found to be stable. The lowest-energy structure of $VGe_{18}$ is $VGe_{18}$-e, in which the V atom is highly coordinated and located at the center of the cage of germanium. However, the isomer $VGe_{18}$-b is found to lie only 0.003 eV/atom above. For n=19, our six best putative isomers are given in Figure 2. As discussed before, the best isomer ($VGe_{19}$-c) combines a prolate-like structure and a cagelike structure. It can be described as a cage-like structure V@$Ge_{11}$ anchored by three Ge atoms to the remainder of the cluster. The binding energy of $VGe_{19}$ is 0.062 eV/atom larger comparatively to the ground state structure of the pure $Ge_{20}$ clusters.

### 3.2. Energetics and electronic properties

To compare the relative stability of the germanium and vanadium doped germanium clusters, the binding energy were calculated as followed:

$$E_b(Ge_{n+1}) = ((n+1)\,E(Ge) - E(Ge_{n+1}))/(n+1),$$
$$E_b(VGe_n) = (n\,E(Ge) + E(V) - E(VGe_n))/(n+1),$$

where *E* represents the total energies of the relevant system. The obtained results are reported in tables 2 and 3. The evolution of binding energies of $Ge_{n+1}$ and $VGe_n$ clusters as a function of the size n is shown in Figure 3 for the most stable isomers. As expected, the binding energy of $Ge_{n+1}$ and $VGe_n$ clusters generally increases with increasing size, which means that these clusters can continuously gain energy during the growth process. For $VGe_n$, the binding energy increases rapidly from 1.19 eV for the dimer to 2.8 eV for cluster with n=6 then a slow and non-monotonic growth is observed up to n= 19, with two local maxima at n=10 and 14. Also, we observe that the binding energy of $VGe_n$ clusters is larger than the corresponding $Ge_{n+1}$ clusters, except for the cases in range of n=3-6. This proves that the doping V atom generally enhances the stability of germanium clusters. This may appear surprising if we consider the binding energy of VGe and $Ge_2$ dimers, 1.198 and 1.446 eV respectively, which seems to be unfavorable to form V-Ge bonds. The great stability is enhanced for the endohedral structures of n=10, 12-15, in which V is encapsulated in a quasi-perfect $Ge_n$ cage. This behavior is due to the absorption of the dangling bonds of the germanium cage by the doping vanadium atom located in a central position. The high binding energies for $VGe_{10}$, $VGe_{12}$, $VGe_{13}$, $VGe_{14}$, and $VGe_{15}$ are calculated to 3.058, 3.127, 3.131, 3.183, 3.179 eV/atom, they are ~0.15 eV/atom larger than those of the corresponding $Ge_{n+1}$ clusters. The highest value of the binding energy is obtained for $VGe_{14}$. The high stability of the $VGe_{14}$ cluster might stem from its high symmetry ($O_h$) and the fact that the enclosed V atom inside the cage of germanium interacts with all germanium atoms (high coordination number).

In order to get insight into the kinetic stability of the clusters, the HOMO–LUMO gap (energy difference between the highest occupied molecular orbital (HOMO) and the lowest unoccupied molecular orbital (LUMO)) of $VGe_n$ clusters was also calculated and analyzed. It is considered to be an important criterion in terms of the electronic stability of clusters and represents the ability for the cluster to participate in chemical reactions. In general as the HOMO-LUMO gap increases, the reactivity of the cluster decreases[53]. The obtained results are shown in Figure 4 for the most stables isomers of each size. For comparison, the HOMO-LUMO gaps of the most stable pure $Ge_{n+1}$ clusters are also reported. Data can be found in Table 2 and 3. The decreasing tendency with increasing size is strong for pure germanium clusters but less significant for $VGe_n$ clusters. The gap of $VGe_n$ is much lower than that of the pure $Ge_{n+1}$ cluster, except for sizes n= 11, 13 and 14, indicating that the vanadium dopant in the germanium clusters generally increases the chemical activity of clusters. The value for $VGe_n$ oscillates roughly between 0.5 and 1 eV but the case n=14 is an exception with a value of 1.495 eV. This points the high stability of $VGe_{14}$ and reflects that this cluster is chemically stable and is a good candidate to be used as a building block for developing new materials.

It is very know in cluster physics that the second order energy difference ($\Delta_2E$) is a sensitive quantity which can directly reflect the relative stability of the corresponding clusters[54]. It is generally compared to the relative concentration of species determined in mass

spectroscopy measurements. Here, the calculated second order energy differences of $Ge_{n+1}$ and $VGe_n$ clusters are obtained as followed

$$\Delta_2 E\,(Ge_{n+1}) = E(Ge_{n+2}) + E(Ge_n) - 2E(Ge_{n+1}),$$
$$\Delta_2 E(VGe_n) = E(VGe_{n+1}) + E(VGe_{n-1}) - 2\,E(VGe_n),$$

and are shown in Figure 05. The large positive value for n= 10 together with the negative values for n=9 and 11 reflect the relative high stability of the opened cage $VGe_{10}$ compared to the exohedral structures of $VGe_9$ and $VGe_{11}$. Similarly, the large positive values for n=12-15 together with the large negative values for n=11 and 16 reflect the high stability of the perfect cages for $VGe_{12\text{-}15}$ compared to the exohedral structure of $VGe_{11}$ and the distorted cage of $VGe_{16}$. It is interesting to note that the $\Delta_2 E$ values for $Ge_{13}$ and $Ge_{16}$ are also large, and so before the substitution of a Ge atom by a V atom (resulting in $VGe_{12}$ and $VGe_{15}$ respectively), the sizes n=12 and 15 are favored. This result indicates that the high stability of $VGe_{12}$ and $VGe_{15}$ might also be due to the high stability of their corresponding initial pure germanium cage $Ge_{13}$ and $Ge_{16}$.

Vertical ionization potential (VIP) and vertical electron affinity (VEA) are defined as:

$$VIP = E^+ - E$$
$$VEA = E - E^-$$

where $E$ is the total energy of the neutral cluster, $E^+$ and $E^-$ represent the total energies of the cationic and anionic clusters respectively with the same geometry as the neutral cluster. These data could be compared to experiment even if to our knowledge no experimental is available nowadays. Results for $Ge_{n+1}$ and $VGe_n$ (n = 1-19) clusters are listed in Tables 2 and 3. The VIP defines the quantity of energy needed to extract an electron from the neutral clusters and it is a useful for determining the stability of clusters. In general, the larger the values of VIP, the more stable is the cluster. Here, the obtained value of VIP for the most stable isomer of $Ge_{n+1}$ and $VGe_n$ clusters are shown in Figure 6. The VIP of $VGe_n$ clusters show an oscillating behavior until size n=14 and a decreasing tendency from n=15. All values are between 6.2 and 7.12 eV. Pronounced peaks are observed at n= 2, 4, 8 and more apparent peak at n= 14. Again, $VGe_{14}$ cluster seems to be particularly stable. The VIP of pure germanium clusters show a decreasing tendency with the increasing of the cluster size, in line with the results obtained for HOMO–LUMO gaps showed in Figure 4. The cluster size dependent of VEA for $Ge_{n+1}$ and $VGe_n$ clusters are plotted in Figure 7. We can see that the electron affinity is sensitive to the size of the cluster and it roughly shows an increasing tendency with the increasing cluster size and thus the larger clusters will capture electrons more easily. The relative minimum located at n=14 indicates a relative larger stability for $VGe_{14}$. Our calculated *VEA* values are found to be 0.4-0.8 eV smaller than the calculated vertical electron detachment energies of the anion $VGe_n^-$. [8]

It has been established that chemical hardness ($\eta$) is an important quantity which may be used to characterize the relative stability of molecules and clusters through the principle of maximum hardness (PMH) of Pearson[55-56]. On the basis of a Koopmans theorem, the chemical hardness $\eta$ is defined as:

$$\eta = VIP - VEA$$

The obtained results are reported in tables 2 and 3 for $Ge_{n+1}$ and $VGe_n$ clusters respectively. The relationships of $\eta$ and the size $n$ are shown in Figure 8 for both species. The chemical hardness has a roughly decreasing evolution as the size $n$ increases for $Ge_{n+1}$ and $VGe_n$ clusters. The relative high value for $VGe_{12\text{-}14}$ indicates a relative high stability for the three clusters, in particular for $VGe_{14}$ for which the value of $\eta$ is as large as for a small cluster like $VGe_4$.

The magnetic behavior of the $VGe_n$ clusters has been investigated by calculating the total spin magnetic moment (TSMM) and the partial density of states (PDOS) 3d, 4s and 4p orbitals for all of the most stables clusters. The TSMM is defined as the difference between the occupation numbers of spin-up and spin-down states. The TSMM values of $VGe_n$ clusters are shown in Table 3 and Figure 9 for the most stables structure in each size. The PDOS are shown in Figure 10 where the Fermi level is shifted to zero position, the spin-down density is plotted as negative and the spin-up density is plotted as positive. We observe that the magnitude of TSMM oscillates between 1 and 5 $\mu_B$. A large TSMM value of 5 $\mu_B$ is observed in clusters with n=1 and 5. For many clusters (n=2,3,4,6,7,9,11,12,14,17,18,19) the value of 3$\mu_B$ is found as for the isolated V atom. The PDOS indicate that the large differences between the up and down electronic states around the Fermi level mainly come from the d states while a very few of magnetic moments are found on the 4s and 4p states. So the magnetic moment of clusters is mainly due to 3d electrons of vanadium. However, the magnetic moment is quenched (1 $\mu_B$) for clusters corresponding to n= 8, 10, 13, 15, 16.

### 3.3. The case $VGe_{14}$

Our results, detailed in previous sections, enhance the high stability of $VGe_{14}$ cluster. The cluster presents the highest stability from both the binding energy (figure 3) and the second-order energy difference (figure 5). It also has a relatively high HOMO-LUMO gap (figure 4), a relatively high VIP (figure 6) and small VEA (figure 7), and a large chemical hardness (Figure 8). Also its geometrical structure adopts the $O_h$ symmetry point group. As a matter of fact, we have checked that all harmonic frequencies are positive, since the lowest ones were calculated to be a $T_{2u}$ mode at 54 $cm^{-1}$ and a $T_{2g}$ mode at 105 $cm^{-1}$. To further investigate that peculiar cluster, we consider the possibility that the high symmetry maximizes the stability by allowing the formation of a quasi-spherically confined free-electron gas inside the cage. The electronic structure of $VGe_{14}$ is detailed in Figure 11. We show the density of states (DOS) and the Kohn-Sham orbitals calculated at PBE/cc-pvtz level with the software Gaussian09 [57]. The 3s and 3p valence electrons of Ge and the 4s and 3d valence electrons of V are found to be delocalized and exhibit a shell structure associated to the quasi-spherical geometry. Although some little deviations from a perfect sphere due to explicit location of atoms and the $O_h$ symmetry instead of $K_h$ (the symmetry of the atom), we can easily distinguish the orbitals S, P, D, F, G. The 61 valence electrons of the cluster are organized with the following occupations: $1S^2\ 1P^6\ 1D^{10}\ 2S^2\ 1F^{14}\ 3S^2\ 2P^6\ 1G^{15}\ 2D^4$. Although the number of electrons does not exactly fit with shell closings numbers, such an organization contributes to the high stability of the cluster through the pooling of electrons. The shell model is well known in metal cluster and has been predicted by the jellium model[58,59] which considers the valence electron confined in a spherically symmetric potential while the ionic core structure is replaced by a uniform positive background. To our knowledge, such an electronic organization in metal-doped germanium clusters has not been previously reported.

Our present results contrast with previous works[7] in which the enhanced stability of $VGe_{15}$ was highlighted and was supposed to originate from a 20-electron filled shell electronic configuration. The analysis was based on the electron counting, where each Ge atom donates one electron to the free-electron gas while V atom gives 5 electrons. Therefore $VGe_{15}$ was a possible 20-electron cluster, and was predicted to have enhanced stability. In our work, an enhanced stability is found for $VGe_{14}$, while $VGe_{15}$ has also a large stability. The stability of $VGe_{14}$ cannot be explained by the 20-electrons rule. The molecular orbitals are clearly in favor of a reorganization of the 61 valence electrons in a super-shell occupations, and not of a 20-electrons rule (or 18-electron as suggested for other metals).

## 4. Conclusion

In this work we have systematically studied the properties of $Ge_{n+1}$ and $VGe_n$ (n = 1-19) clusters using first principles DFT calculations. The lowest energy structures and some low lying isomers have been identified for both pure and vanadium doped germanium clusters. In optimized structures of pure germanium clusters, Ge atoms are generally localized at the surface of the cluster. Up to n=9, $VGe_n$ clusters adopt a somewhat similar structure than their corresponding $Ge_{n+1}$, except $VGe_3$ and $VGe_8$. For $n \geq 10$ the endohedrally vanadium doped germanium structures are predicted to be the most stable. For n=10-16, the vanadium atom forms a core surrounded by all Ge atoms which in turn form an opened cage for n=10 and 11 and a fully closed cage for n=12-16 in which V is encapsulated. Then, for larger size, we see a competition between some prolate- and cage-like structures. For $VGe_{19}$, the best isomer combines a prolate-like structure and a cagelike structure. It can be described as a cage-like structure V@Ge11 anchored by three Ge atoms to the remainder of the cluster. Hence, we can expect similar features for larger size $VGe_n$ clusters with a cage-like $V@Ge_n$, n~14, anchored to the other germanium atoms.

The dopant V atom in the $Ge_n$ clusters has not an immediate effect on the stability of small germanium clusters (n<6) but it contributes largely to strengthen the stabilities of the germanium cages from n=10 to n=19. The HOMO–LUMO gaps of the $VGe_n$ clusters are generally smaller than those of the corresponding $Ge_{n+1}$ clusters. The calculated binding energy, the second-order energy difference, the HOMO–LUMO gaps, vertical ionization potential, chemical hardness manifest the large stability of the $VGe_{14}$ cluster with $O_h$ symmetry. That cluster presents a peculiar electronic structure in which the valence electrons of V and Ge atoms are delocalized and exhibit a shell structure associated to the quasi-spherical geometry. Consequently, this cluster can be a good candidate to be used as the building blocks for developing new materials. The Mulliken electrons population analysis explored in the partial density of states (PDOS) indicates that the total spin magnetic moment of $VGe_n$ clusters is mainly due to 3d electrons.

**Acknowledgement**

FR thanks the Pôle Scientifique de Modélisation Numérique (PSMN) at Lyon, France, and the GENCI-IDRIS (Grant i2016086864) center for generous allocation of computational time.

**References**

[01] Jackson, K.; Nellermoe, B. Zr@Si20: A Strongly Bound Si Endohedral System, *Chem. Phys. Lett.* **1996**, *254*, 249-256.

[02] Hiura, H.; Miyazaki, T.; Kanayama, T. Formation of Metal-Encapsulating Si Cage Clusters, *Phys. Rev. Lett*. **2001**, *86*, 1733-1736.

[03] Kumar V.; Kawazoe, Y. Metal-Encapsulated Fullerenelike and Cubic Caged Clusters of Silicon, *Phys. Rev. Lett*. **2001**, *87*, 045503.

[04] Sporea, C.; Rabilloud, F. Stability of Alkali-Encapsulating Silicon Cage Clusters, *J. Chem. Phys.* **2007**, *127*, 164306.

[05] Xia, X. X.; Hermann,A.; Kuang, X.Y.; Jin, Y.Y.; Lu, C.; Xing, X.D; Study of the Structural and Electronic Properties of Neutral and Charged Niobium-Doped Silicon Clusters: Niobium Encapsulated in Silicon Cages, *J. Phys. Chem. C* **2016**, *120*, 677-684.

[06] Han, J.G. ; Hagelberg, F., Recent Progress in the Computational Study of Silicon and Germanium Clusters with Transition Metal Impurities *J. Comput. Theor. Nanosci.*, **2009**, *6*, 257-269.

[07] Bandyopadhyay, D.; Kaur, P.; Sen, P. New Insights into Applicability of Electron-Counting Rules in Transition Metal Encapsulating Ge Cage Clusters, *J. Phys. Chem. A* **2010**, *114*, 12986–12991.

[08] Deng, X.-J.; Kong, X.-Y.; Xu, H.-G.; Xu, X.-L.; Feng, G.; Zheng, W.-J., Photoelectron Spectroscopy and Density Functional Calculations of $VGe_n^-$ (n = 3−12) Clusters, *J. Phys. Chem. C* **2015**, *119*, 11048-11055.

[09] Jin, Y.; Tain, Y.; Kuang, X.; Lu, C.; Cabellos, J. L., Mondal, S.; Merino, G. Structural and Electronic Properties of Ruthenium-Doped Germanium Clusters, *J. Phys. Chem. C*, **2016**, *120*, 8399-8404.

[10] Bulusu, S.; Yoo, S.; Zeng, X.C. Search for Global Minimum Geometries for Medium Sized Germanium Clusters: $Ge_{12}$–$Ge_{20}$, *J. Chem. Phys*. **2005**, *122*, 164305.

[11] Wang, J.; Han, J.G. A Computational Investigation of Copper-Doped Germanium and Germanium Clusters by the Density-Functional Theory, *J. Chem. Phys*. **2005**, *123*, 244303.

[12] Yoo, S.; Zeng, X.C. Search for Global-Minimum Geometries of Medium-Sized Germanium Clusters. II. Motif-Based Low-Lying Clusters $Ge_{21}$ – $Ge_{29}$, *J. Chem. Phys*. **2006**, *124*, 184309.

[13] Wang L.; Zhao, J. Competition Between Supercluster and Stuffed Cage Structures in Medium-Sized $Ge_n$ (n = 30 – 39) clusters, *J. Chem. Phys*. **2008**, *128*, 024302.

[14] Wielgus, P.; Roszak, S.; Majumdar, D.; Saloni, J.; Leszczynski, J. Theoretical Studies on the Bonding and Thermodynamic Properties of $Ge_nSi_m$ ( m + n= 5 ) Clusters: The Precursors of Germanium/Silicon Nanomaterials, *J. Chem. Phys*. **2008**, *128*, 144305.

[15] Jing, Q.; Tian, F.; Wang, Y. No Quenching of Magnetic Moment for the $Ge_nCo$ (n=1 – 13) Clusters: First Principles Calculations, *J. Chem. Phys*. **2008**, *128*, 124319.

[16] Deng, X.J.; Kong, X.Y.; Xu, X.L.; Xu, H.G.; Zheng, W.J. Structural and Magnetic Properties of $CoGe_n^-$ (n=2–11) Clusters: Photoelectron Spectroscopy and Density Functional Calculations, *Chem. Phys. Chem*. **2014**, *15*, 3987 – 3993.

[17] Kumar, M.; Bhattacharyya N.; Bandyopadhyay, D. Architecture, Electronic Structure and Stability of $TM@Ge_n$ (TM = Ti, Zr and Hf; n = 1-20) Clusters: a Density Functional Modeling, *J. Mol. Model.* **2012**, *18*, 405–418.

[18] Bandyopadhyay, D. Architectures, Electronic Structures, and Stabilities of Cu-doped $Ge_n$ Clusters: Density Functional Modeling, *J. Mol. Model*. **2012**, *18*, 3887–3902.
[19] King, R.B.; Silaghi-Dumitrescu I.; Lupan, A. Density Functional Theory Study of Eight-Atom Germanium Clusters: Effect of Electron Count on Cluster Geometry, *Dalton Trans.* **2005**, 1858 – 1864.
[20] King, R.B.; Silaghi-Dumitrescu, I.; Density Functional Theory Study of Nine-Atom Germanium Clusters: Effect of Electron Count on Cluster Geometry, *Inorg. Chem.* **2003**, *42*, 6701-6708.
[21] Singh, A. K.; Kumar, V.; Kawazoe, Y. Thorium Encapsulated Caged Clusters of Germanium: Th@$Ge_n$, n= 16, 18, and 20, *J. Phys. Chem. B*, **2005**, *109*, 15187-15189.
[22] Wang, J.; Han, J.G. A Theoretical Study on Growth Patterns of Ni-Doped Germanium Clusters, *J. Phys. Chem. B* **2006**, *110*, 7820-7827.
[23] Wang, J.; Han, J.G. Geometries and Electronic Properties of the Tungsten-Doped Germanium Clusters: W$Ge_n$ (n = 1-17) *J. Phys. Chem. A* **2006**, *110*, 12670-12677.
[24] Wang, J.; Han, J.G Geometries, Stabilities, and Vibrational Properties of Bimetallic $Mo_2$-Doped $Ge_n$ (n = 9-15) Clusters: A Density Functional Investigation, *J. Phys. Chem. A* **2008**, *112*, 3224-3230.
[25] Zhao, L.Z.; Lu, W.C.; Qin, W.; Wang, C.Z.; Ho, K.M. Comparison of the Growth Patterns of $Si_n$ and $Ge_n$ Clusters (n = 25-33), *J. Phys. Chem. A* **2008**, *112*, 5815–5823.
[26] Gopakumar, G.; Ngan, V.T.; Lievens, P.; Nguyen, M.T. Electronic Structure of Germanium Monohydrides $Ge_nH$, n = 1-3, *J. Phys. Chem. A* **2008**, *112*, 12187–12195.
[27] Zdetsis, A.D. Silicon-Bismuth and Germanium-Bismuth Clusters of High Stability, *J. Phys. Chem. A* **2009**, *113*, 12079–12087.
[28] Bandyopadhyay D.; Sen, P. Density Functional Investigation of Structure and Stability of Gen and $Ge_nNi$ (n = 1-20) Clusters: Validity of the Electron Counting Rule, *J. Phys. Chem. A* **2010**, *114*, 1835–1842.
[29] Nagendran, S.; Sen, S.S.; Roesky, H.W.; Koley, D.; Grubmüller, H.; Pal A.; Herbst-Irmer, R. RGe(I) Ge(I)R Compound (R = $PhC(NtBu)_2$) with a Ge-Ge Single Bond and a Comparison with the Gauche Conformation of Hydrazine, *Organometallics* **2008**, *27*, 5459–5463.
[30] Shi, S.; Liu, Y.; Zhang, C.; Deng B.; Jiang, G. A Computational Investigation of Aluminum-Doped Germanium Clusters by Density Functional Theory Study, *Comp. Theo. Chem.* **2015**, *1054*, 8–15.
[31] Islam M.S.; Ray, A.K. Many-body Perturbation Theory Applied to Small Germanium Clusters, *Chem. Phys. Lett.* **1998**, *153*, 496-502.
[32] Deutsch, P.W.; Curtiss L.A.; Blaudeau, J.P. Electron Affinities of Germanium Anion Clusters, $Ge_n^-$ (n=2-5), *Chem. Phys. Lett*. **2001**, *344*, 101-106.
[33] Deutsch, P.W.; Curtiss L.A.; Blaudeau, J.P. Binding Energies of Germanium Clusters, $Ge_n$ (n = 2-5), *Chem. Phys. Lett.* **1997**, *270*, 413-418.
[34] Kapila, N.; Garg, I.; Jindal, V.K.; Sharma, H. First Principle Investigation into Structural Growth and Magnetic Properties in $Ge_nCr$ Clusters for n=1–13, *J. Magn. and Magn. Mat.* **2012**, *324*, 2885–2893.
[35] Sosa-Hernandez, E.M.; Alvarado-Leyva, P.G. Magnetic Properties of Stable Structures of Small Binary $Fe_nGe_m$ ($n + m \leq 4$) Clusters, *Physica E* **2009**, *42*, 17–21.
[36] Li, X.; Su, K.; Yang, X.; Song L.; Yang, L. Size-Selective Effects in the Geometry and Electronic Property of Bimetallic Au–Ge Nanoclusters, *Comp. Theo. Chem.* **2013**, *1010*, 32–37.
[37] Kapila, N.; Jindal V.K.; Sharma, H. Structural, Electronic and Magnetic Properties of Mn, Co, Ni in $Ge_n$ for (n=1–13), *Physica B* **2011**, *406*, 4612–4619.

[38] Zhao, W.J.; Wang, Y.X. Geometries, Stabilities, and Magnetic Properties of $MnGe_n$ (n = 2–16) Clusters: Density-Functional Theory Investigations, *J. Mol. Struct.: THEOCHEM* **2009**, *901*, 18–23.
[39] Bals, S.; Van Aert, S.; Romero, C.P.; Lauwaet, K.; Van Bael, M.J.; Schoeters, B.; Partoens, B.; Yücelen, E.; Lievens P.; Van Tendeloo, G. Atomic Scale Dynamics of Ultrasmall Germanium Clusters, *Nat. Comm.* **2012**, *3*, 897.
[40] Hou, X.J.; Gopakumar, G.; Lievens P.; Nguyen, M.T. Chromium-Doped Germanium Clusters $CrGe_n$ (n = 1-5): Geometry, Electronic Structure, and Topology of Chemical Bonding, *J. Phys. Chem. A* **2007**, *111*, 13544-13553.
[41] Samanta P.N.; Das, K.K.; Electronic Structure, Bonding, and Properties of $Sn_mGe_n$ (m + n ≤ 5) Clusters: A DFT Study, *Comp. Theo Chem* **2012**, *980*, 123-132.
[42] Zhao, W.J.; Wang, Y.X. Geometries, Stabilities, and Electronic Properties of $FeGe_n$ (n = 9-16) Clusters: Density-Functional Theory Investigations, *Chem. Phys.* **2008**, *352*, 291-296.
[43] Liang F.S.; Li, B.X. Stable Structures of $Ge_n$ (n = 21–25) Clusters, *Phys. Lett. A* **2004**, *328*, 407–413.
[44] Mahtout, S.; Tariket, Y. Electronic and Magnetic Properties of $CrGe_n$ ($15 \leq n \leq 29$) Clusters: A DFT Study, *Chem Phys* **2016**, *472*, 270–277.
[45] Soler, J.M.; Artacho, E.; Gale, J.D.; García, A.; Junquera, J.; Ordejón, P.; Sánchez-Portal, D. The SIESTA Method for Ab Initio Order-N Materials Simulation *J. Phys.: Cond. Matt*. **2002**, *14*, 2745-2779.
[46] Perdew, J.P.; Burke, K.; Ernzerhof, M. Generalized Gradient Approximation Made Simple, *Phys. Rev. Lett*. **1996**, *77*, 3865-3868.
[47] Troullier N.; Martins, J.L. Efficient Pseudopotentials for Plane-Wave Calculations, *Phys. Rev. B* **1991**, *43*, 1993-2006.
[48] Kleinman L.; Bylander, D.M. Efficacious Form for Model Pseudopotentials, *Phys. Rev. Lett.* **1982**, *48*, 1425-1428.
[49] Kohn W.; Sham, L.J. Self-Consistent Equations Including Exchange and Correlation Effects, *Phys. Rev. A* **1965**, *140*, 1133-1138.
[50] Kingcade, J.E.; Nagarathna-Naik, H. M.; Shim, I.; Gingerich, K. A.; Electronic Structure and Bonding of the Molecule $Ge_2$ from All-Electron Ab Initio Calculations and Equilibrium Measurements, J. Phys. Chem. **1986**, *90*, 2830-2834.
[51] Gadiyak, G.V.; Morokov, Y.N.; Mukhachev, A.G. and Chernov, S.V.; Electron Density Functional Method for Molecular System Calculations, Zh. Strukt. Khim. **1981**, *22*, 36-40.
[52] Shim, I. M.; Baba, S.; and Ginerich, K.; Electronic Structure of $Ge_2$ and $Ge_2^-$ and Thermodynamic Properties of $Ge_2$ from All Electron Ab Initio Investigations and Knudsen Effusion Mass Spectroscopic Measurements, Chem. Phys. **2002,** *277*, 9-20.
[53] Yoshida M.; Aihara, J.I. Validity of the Weighted HOMO–LUMO Energy Separation as an Index of Kinetic Stability for Fullerenes with up to 120 Carbon Atoms, *Phys. Chem. Chem. Phys.* **1999**, *1*, 227-230.
[54] Wang, J.L.; Wang, G.H; Zhao, J.J. Structure and Electronic Properties of $Ge_n$ (n = 2–25) Clusters from Density-Functional Theory, *Phys. Rev. B* **2001**, *64*, 205411–205415.
[55] Parr R.G.; Yang, W. Density Functional Theory of Atoms and Molecules. New York: Oxford University Press (1989).
[56] Parr R.G.: Pearson. R.G. Absolute Hardness: Companion Parameter to Absolute Electronegativity, *J Am. Chem. Soc.* **1983**, *105*, 7512-7516.
[57] Frisch M.J.; Trucks, G.W.; Schlegel, H.B.; Scuseria, G.E.; Robb, M.A.; Cheeseman, J.R.; Scalmani, G.; Barone, V.; Petersson, G.A.; Nakatsuji, H., et al., Gaussian09, Revision D.01, Gaussian Inc., Wallingford CT, 2013.
[58] de Heer, W.A. The Physics of Simple Metal Clusters: Experimental Aspects and Simple Models, *Rev. Mod. Phys*. **1993**, *65*, 611-676.

[59] Brack, M. The Physics of Simple Metal Clusters: Self-Consistent Jellium Model and Semiclassical Approaches, *Rev. Mod. Phys.* **1993**, *65*, 677-732.

**Table 1:** The binding energy and bond length of $Ge_2$ dimers: comparisons with other available experimental and theoretical data.

| Parameters | Our work | Theoretical value | Experimental value |
|---|---|---|---|
| $E_b$ (eV/atom) | 1.446 | 1.44 [a], 1.772[e], 1.92[k], 1.34[l], ~1.45[i] | 1.35[m] |
| R (Å) | 2.450 | 2.548[a], 2.399 [b], 2.54[c], 2.421[e], 2.528[d], 2.413[f], 2.36[g], 2.375[h], 2.48[j], 2.44[l], 2.422[p] | 2.57[n]. 2.44[o] |

[a] Ref. [11].
[b] Ref. [14].
[c] Ref. [18].
[d] Ref. [23].
[e] Ref. [24].
[f] Ref. [30].
[g] Ref. [31].
[h] Ref. [33].
[i] Ref. [34].
[j] Ref. [35].
[k] Ref. [37].
[l] Ref. [40].
[m] Ref. [50].
[n] Ref. [29].
[o] Ref. [51].
[p] Ref. [52].

**Table 2:** Symmetry group, binding energy $E_b$ (eV/atom), HOMO-LUMO gap ΔE (eV), vertical ionization potential VIP (eV), vertical electron affinity VEA (eV) and chemical hardness $\eta$ (eV) for $Ge_{n+1}$ (n=1-19) clusters.

| n | Symmetry | $E_b$ (*eV/atom*) | ΔE (*eV*) | VIP (*eV*) | VEA (*eV*) | $\eta$ *(eV)* | $a_{Ge-Ge}$ |
|---|---|---|---|---|---|---|---|
| **1** | a- $D_{\infty h}$ | 1.446 | 1.816 | 7.844 | 1.900 | 5.944 | 2.450 |
| **2** | a- $D_{\infty h}$ | 2.049 | 1.267 | 7.789 | 1.427 | 6.362 | 2.342 |
| | **b-$D_{3h}$** | **2.059** | 2.426 | **7.804** | **2.200** | **5.604** | **2.546** |
| **3** | a-$C_{2v}$ | 2.212 | 0.207 | 7.197 | 2.046 | 5.151 | 2.502 |
| | **b-$D_{2h}$** | **2.556** | **1.179** | **7.855** | **1.558** | **6.298** | **2.577** |
| | c-$D_{2d}$ | 2.277 | 1.067 | 7.243 | 2.230 | 5.013 | 2.517 |
| **4** | a-$C_{4v}$ | 2.490 | 0.643 | 7.664 | 2.176 | 5.488 | 2.668 |
| | **b-$D_{3h}$** | **2.707** | **2.068** | **8.062** | **1.213** | **6.849** | **2.548** |
| **5** | **a-$D_{4h}$** | **2.847** | **1.995** | **7.863** | **1.269** | **6.594** | **2.783** |
| | b-$C_s$ | 2.739 | 0.925 | 7.474 | 1.952 | 5.522 | 2.703 |
| | **c- $C_s$** | **2.848** | **1.957** | **7.828** | **1.251** | **6.577** | **2.744** |
| **6** | **a- $D_{5h}$** | **2.975** | **1.836** | **7.939** | **1.700** | **6.239** | **2.747** |
| | b- $C_{2v}$ | 2.695 | 0.243 | 6.952 | 2.428 | 4.524 | 2.757 |
| | c- $C_s$ | 2.700 | 0.292 | 6.849 | 2.278 | 4.571 | 2.772 |
| | d- $C_2$ | 2.844 | 1.171 | 7.169 | 1.657 | 5.512 | 2.755 |
| **7** | a- $C_{2v}$ | 2.867 | 0.980 | 7.300 | 2.157 | 5.143 | 2.777 |
| | **b-1- $C_s$** | **2.903** | **1.214** | **7.122** | **1.714** | **5.407** | **2.762** |
| | c-2- $C_s$ | 2.782 | 1.057 | 7.064 | 1.915 | 5.149 | 2.721 |
| | d- $C_{2v}$ | 2.838 | 1.197 | 7.233 | 1.897 | 5.335 | 2.768 |
| **8** | **a- $C_{4v}$** | **2.874** | **1.360** | **7.258** | **1.915** | **5.343** | **2.663** |
| | b- $D_{3h}$ | 2.716 | 0.397 | 6.817 | 2.600 | 4.217 | 2.690 |
| | c- $C_{2v}$ | 2.675 | 0.508 | 6.783 | 2.401 | 4.382 | 2.787 |
| | d- $C_{2v}$ | 2.837 | 0.898 | 6.972 | 2.087 | 4.885 | 2.826 |
| **9** | a- $D_{2h}$ | 2.947 | 1.293 | 7.139 | 1.948 | 5.191 | 2.766 |
| | b- $D_{4h}$ | 2.735 | 0.001 | 6.551 | 2.678 | 3.873 | 2.740 |
| | **c- $C_1$** | **2.953** | **1.297** | **7.013** | **1.851** | **5.162** | **2.748** |
| | d- $C_1$ | 2.895 | 1.106 | 6.936 | 1.980 | 4.956 | 2.771 |
| | e- $C_{2v}$ | 2.846 | 0.997 | 6.933 | 2.077 | 4.855 | 2.686 |
| **10** | a- $C_s$ | 2.928 | 0.807 | 6.850 | 2.330 | 4.520 | 2.786 |
| | b- $C_2$ | 2.954 | 1.229 | 6.784 | 1.837 | 4.946 | 2.758 |
| | **c- $C_{2v}$** | **2.959** | **0.861** | **6.923** | **2.339** | **4.584** | **2.839** |
| | d- $C_{2v}$ | 2.850 | 1.051 | 6.643 | 1.965 | 4.679 | 2.695 |
| **11** | a- $C_{2h}$ | 2.976 | 0.578 | 6.586 | 2.390 | 4.195 | 2.755 |
| | b- $D_{2h}$ | 2.899 | 0.491 | 6.839 | 2.690 | 4.149 | 2.706 |
| | c- $D_{4h}$ | 2.872 | 0.268 | 6.928 | 2.986 | 3.942 | 2.787 |
| | d- $C_s$ | 2.886 | 0.754 | 6.847 | 2.507 | 4.340 | 2.738 |
| | e- $C_1$ | 2.935 | 0.913 | 6.641 | 2.123 | 4.517 | 2.795 |
| | **f- $C_{2v}$** | **2.979** | **0.442** | **6.689** | **2.517** | **4.171** | **2.817** |
| **12** | a- $C_{2v}$ | 2.824 | 0.159 | 6.129 | 2.373 | 3.756 | 2.885 |
| | b- $C_{4v}$ | 2.917 | 0.708 | 6.998 | 2.687 | 4.311 | 2.824 |
| | c- $C_1$ | 2.984 | 1.095 | 6.902 | 2.268 | 4.634 | 2.771 |
| | **d- $C_1$** | **2.994** | **1.127** | **6.978** | **2.318** | **4.660** | **2.721** |
| | e- $C_1$ | 3.010 | 1.127 | 6.906 | 2.299 | 4.607 | 2.811 |
| **13** | a- $O_h$ | 2.940 | 1.888 | 7.149 | 3.608 | 3.541 | 2.810 |
| | **b- $C_1$** | **2.987** | **0.812** | **6.472** | **2.238** | **4.234** | **2.725** |
| | c- $C_1$ | 2.970 | 1.138 | 6.675 | 2.220 | 4.455 | 2.752 |
| | d- $C_1$ | 2.952 | 0.853 | 6.636 | 2.395 | 4.240 | 2.753 |
| | e- $C_1$ | 2.955 | 0.791 | 6.528 | 2.295 | 4.233 | 2.832 |
| | f- $C_1$ | 2.948 | 0.953 | 6.633 | 2.337 | 4.296 | 2.781 |
| **14** | a- $O_h$ | 2.912 | 0.525 | 6.135 | 2.278 | 3.857 | 2.873 |
| | **b- $C_1$** | **3.018** | **1.108** | **6.679** | **2.207** | **4.472** | **2.772** |
| | **c- $C_1$** | **3.019** | **0.958** | **6.856** | **2.514** | **4.342** | **2.791** |
| | e- $C_1$ | 2.955 | 0.848 | 6.394 | 2.256 | 4.138 | 2.737 |
| | f- $C_s$ | 2.964 | 1.136 | 6.689 | 2.177 | 4.512 | 2.726 |
| **15** | **a- $D_{2h}$** | **3.052** | **1.106** | **6.661** | **2.278** | **4.383** | **2.759** |
| | b- $C_s$ | 2.980 | 0.900 | 6.627 | 2.415 | 4.212 | 2.751 |
| | c- $C_{2v}$ | 3.022 | 0.594 | 6.467 | 2.519 | 3.948 | 2.829 |
| | d- $C_1$ | 2.982 | 1.172 | 6.824 | 2.347 | 4.477 | 2.794 |
| | e- $C_1$ | 2.976 | 0.935 | 6.526 | 2.392 | 4.134 | 2.732 |
| **16** | **a- $C_s$** | **3.010** | **0.719** | **6.584** | **2.682** | **3.902** | **2.805** |
| | b- $C_2$ | 2.959 | 0.541 | 6.442 | 2.774 | 3.668 | 2.792 |
| | c- $C_1$ | 2.990 | 1.130 | 6.597 | 2.302 | 4.295 | 2.797 |
| **17** | a- $C_{2v}$ | 2.948 | 0.671 | 6.420 | 2.554 | 3.866 | 2.821 |
| | **b- $C_2$** | **3.046** | **0.777** | **6.531** | **2.599** | **3.932** | **2.732** |
| | c- $C_1$ | 2.990 | 0.991 | 6.518 | 2.415 | 4.103 | 2.772 |
| | d- $C_s$ | 2.976 | 0.693 | 6.619 | 2.827 | 3.792 | 2.764 |
| | e- $C_s$ | 2.942 | 0.274 | 6.265 | 2.823 | 3.442 | 2.726 |
| **18** | **a- $C_{2v}$** | **3.054** | **1.074** | **6.811** | **2.617** | **4.194** | **2.769** |
| | b- $C_1$ | 3.039 | 0.829 | 6.392 | 2.450 | 3.942 | 2.766 |
| | c- $C_1$ | 3.017 | 1.065 | 6.652 | 2.543 | 4.109 | 2.728 |
| | d- $C_{3v}$ | 3.024 | 1.255 | 6.504 | 2.168 | 4.336 | 2.748 |

| | | | | | | | |
|---|---|---|---|---|---|---|---|
| **19** | a- $C_{2v}$ | 3.004 | 0.606 | 6.363 | 2.710 | 3.653 | 2.743 |
| | **b- $C_1$** | **3.054** | **0.812** | **6.480** | **2.640** | **3.840** | **2.812** |
| | c- $C_1$ | 3.032 | 0.590 | 6.399 | 2.766 | 3.633 | 2.733 |
| | d- $D_{2h}$ | 2.956 | 0.243 | 6.198 | 3.014 | 3.184 | 2.611 |
| | e- $C_{2h}$ | 3.002 | 0.303 | 6.514 | 3.236 | 3.278 | 2.653 |

**Table 3:** Symmetry group, binding energy $E_b$ (eV), HOMO-LUMO gap ΔE (eV), total spin magnetic moment μ ($\mu_b$), vertical ionization potential VIP (eV) and electron affinity VEA (eV), chemical hardness $\eta$ (eV) and bond length $a_{(Ge\text{-}Ge.\ Ge\text{-}V)}$ (Å) for $VGe_n$ (n=1-19) clusters.

| n | Symmetry | $E_b$ (*eV*) | ΔE (*eV/atom*) | μ ($\mu_B$) | VIP (*eV*) | VEA (*eV*) | *η(eV)* | $a_{Ge\text{-}Ge}$ | $a_{Ge\text{-}V}$ |
|---|---|---|---|---|---|---|---|---|---|
| **1** | a- $C_{\infty v}$ | 1.198 | 0.746 | 4.999 | 6.257 | 0.608 | 5.648 | - | 2.526 |
| **2** | a- $D_{\infty h}$ | 1.450 | 0.922 | 8.909 | 6.786 | 1.595 | 5.191 | - | 2.588 |
| | **b- $C_{2v}$** | **2.159** | **0.942** | **3.000** | **6.938** | **0.845** | **6.093** | **2.405** | **2.536** |
| **3** | a- $C_{2v}$ | 2.330 | 0.747 | 4.999 | 6.392 | 1.369 | 5.023 | 2.423 | 2.684 |
| | **b- $C_{3v}$** | **2.350** | **0.533** | **2.999** | **6.352** | **0.927** | **5.425** | **2.676** | **2.599** |
| **4** | **a- $C_s$** | **2.560** | **0.606** | **2.999** | **6.820** | **1.515** | **5.305** | **2.713** | **2.600** |
| | b- $C_{2v}$ | 2.409 | 0.186 | 4.988 | 6.747 | 2.275 | 4.472 | 2.496 | 2.696 |
| | c- $C_{2v}$ | 2.347 | 0.430 | 3.000 | 5.937 | 1.337 | 4.600 | 2.580 | 2.493 |
| | d- $C_{3v}$ | 2.494 | 0.306 | 0.999 | 6.625 | 1.736 | 4.889 | 2.746 | 2.588 |
| **5** | a- $C_s$ | 2.620 | 0.908 | 3.000 | 6.528 | 1.657 | 4.871 | 2.577 | 2.655 |
| | b- $C_s$ | 2.602 | 0.499 | 4.953 | 6.361 | 1.930 | 4.431 | 2.726 | 2.679 |
| | **c- $C_{2v}$** | **2.733** | **0.726** | **4.997** | **6.648** | **1.817** | **4.831** | **2.704** | **2.770** |
| | d- $C_1$ | 2.694 | 0.730 | 3.000 | 6.916 | 1.932 | 4.983 | 2.699 | 2.573 |
| **6** | **a- $C_{2v}$** | **2.838** | **0.363** | **3.000** | **6.392** | **1.745** | **4.647** | **2.746** | **2.750** |
| | b- $C_{2v}$ | 2.686 | 0.341 | 2.999 | 6.687 | 2.288 | 4.399 | 2.655 | 2.820 |
| | c- $C_1$ | 2.769 | 0.495 | 4.996 | 6.039 | 1.696 | 4.343 | 2.737 | 2.802 |
| | **d- $C_{3v}$** | **2.837** | **0.913** | **2.999** | **6.891** | **1.846** | **5.046** | **2.494** | **2.816** |
| **7** | a- $C_{3v}$ | 2.822 | 0.591 | 1.001 | 6.446 | 2.017 | 4.429 | 2.586 | 2.805 |
| | **b- $C_s$** | **2.905** | **0.842** | **3.000** | **6.666** | **1.936** | **4.730** | **2.713** | **2.837** |
| | c- $C_s$ | 2.777 | 0.294 | 2.999 | 6.861 | 2.569 | 4.292 | 2.765 | 2.717 |
| | d- $C_{2v}$ | 2.823 | 0.596 | 0.999 | 6.806 | 2.321 | 4.485 | 2.734 | 2.597 |
| **8** | a- $C_s$ | 2.906 | 0.616 | 3.000 | 6.632 | 2.200 | 4.432 | 2.757 | 2.731 |
| | b- $C_{2v}$ | 2.765 | 0.393 | 2.998 | 6.790 | 2.620 | 4.170 | 2.663 | 2.591 |
| | c- $C_{2v}$ | 2.738 | 0.575 | 2.999 | 6.923 | 2.637 | 4.286 | 2.649 | 2.717 |
| | **d- $C_{2v}$** | **2.966** | **0.570** | **1.000** | **7.043** | **2.727** | **4.316** | **2.758** | **2.809** |
| **9** | a- $C_s$ | 2.952 | 0.833 | 2.999 | 6.643 | 2.029 | 4.614 | 2.797 | 2.685 |
| | b- $C_{4v}$ | 2.826 | 0.485 | 4.899 | 6.185 | 2.092 | 4.093 | 2.702 | 2.675 |
| | c- $C_1$ | 2.953 | 0.537 | 2.999 | 6.648 | 2.459 | 4.189 | 2.712 | 2.786 |
| | d- $C_1$ | 2.884 | 0.444 | 3.000 | 6.372 | 2.339 | 4.032 | 2.786 | 2.755 |
| | **e- $C_s$** | **2.996** | **0.651** | **3.000** | **6.663** | **2.244** | **4.419** | **2.768** | **2.773** |
| | f- $C_1$ | 2.992 | 0.621 | 1.002 | 6.910 | 2.868 | 4.042 | 2.765 | 2.809 |
| **10** | a- $C_1$ | 2.924 | 0.564 | 3.000 | 6.451 | 2.189 | 4.262 | 2.775 | 2.695 |
| | b- $C_1$ | 2.977 | 0.492 | 3.000 | 6.321 | 2.311 | 4.010 | 2.786 | 2.714 |
| | **c- $C_{2v}$** | **3.058** | **0.609** | **1.000** | **6.727** | **2.603** | **4.124** | **2.827** | **2.766** |
| | d- $C_1$ | 2.913 | 0.402 | 3.001 | 6.172 | 2.357 | 3.815 | 2.736 | 2.779 |
| **11** | **a- $C_{2v}$** | **3.024** | **0.446** | **2.991** | **6.560** | **2.817** | **3.744** | **2.689** | **2.920** |
| | b- $C_s$ | 2.951 | 0.831 | 4.999 | 5.981 | 2.010 | 3.971 | 2.660 | 2.630 |
| | c- $C_s$ | 2.992 | 0.698 | 1.010 | 6.526 | 2.789 | 3.737 | 2.750 | 2.871 |
| | d- $C_1$ | 2.984 | 0.676 | 2.999 | 6.378 | 2.214 | 4.164 | 2.750 | 2.812 |
| | e- $C_{2v}$ | 2.977 | 0.513 | 3.000 | 6.452 | 2.483 | 3.969 | 2.804 | 2.721 |
| **12** | a- $C_{2v}$ | 3.018 | 0.560 | 3.003 | 6.948 | 3.152 | 3.796 | 2.772 | 2.914 |
| | b- $C_1$ | 3.036 | 0.733 | 3.000 | 6.739 | 2.615 | 4.124 | 2.775 | 2.873 |
| | c- $C_1$ | 3.034 | 0.674 | 2.999 | 6.801 | 2.728 | 4.073 | 2.790 | 2.811 |
| | d- $C_s$ | 3.108 | 0.712 | 2.999 | 6.816 | 2.685 | 4.131 | 2.792 | 2.879 |
| | e- $D_{4h}$ | 3.071 | 0.711 | 3.000 | 6.919 | 2.632 | 4.287 | 2.747 | 2.902 |
| | **f- $D_{3d}$** | **3.127** | **0.813** | **2.999** | **6.919** | **2.693** | **4.226** | **2.612** | **2.899** |
| **13** | **a- $C_{6v}$** | **3.131** | **1.001** | **1.000** | **6.763** | **2.366** | **4.397** | **2.695** | **2.889** |
| | b- $C_{2v}$ | 3.029 | 0.675 | 2.999 | 6.445 | 2.439 | 4.006 | 2.765 | 2.814 |
| | c- $C_1$ | 3.047 | 0.629 | 1.000 | 6.494 | 2.828 | 3.666 | 2.739 | 2.845 |
| | d- $C_1$ | 3.019 | 0.386 | 2.999 | 6.333 | 2.649 | 3.684 | 2.763 | 2.840 |
| **14** | **a- $O_h$** | **3.183** | **1.495** | **2.999** | **7.120** | **2.297** | **4.823** | **2.693** | **2.913** |
| | b- $D_{6h}$ | 3.100 | 0.642 | 2.999 | 6.488 | 2.491 | 3.997 | 2.780 | 2.920 |
| | c- $C_1$ | 3.027 | 0.320 | 3.000 | 6.023 | 2.544 | 3.479 | 2.692 | 2.901 |
| | d- $C_s$ | 3.110 | 0.333 | 3.000 | 6.494 | 2.925 | 3.569 | 2.625 | 2.944 |
| **15** | a- $C_1$ | 3.099 | 0.519 | 3.000 | 6.491 | 2.784 | 3.707 | 2.778 | 2.878 |
| | b- $C_1$ | 3.026 | 0.530 | 3.000 | 6.490 | 2.762 | 3.728 | 2.781 | 2.682 |
| | **c- $C_s$** | **3.179** | **0.469** | **1.000** | **6.532** | **2.760** | **3.772** | **2.755** | **3.005** |
| | d- $C_1$ | 3.067 | 0.701 | 3.000 | 6.376 | 2.660 | 3.716 | 2.755 | 2.890 |
| | e- $C_1$ | 3.062 | 0.557 | 3.000 | 6.383 | 2.645 | 3.738 | 2.776 | 2.918 |
| **16** | a- $D_{2h}$ | 3.052 | 0.442 | 1.000 | 6.674 | 3.047 | 3.627 | 2.749 | 3.025 |
| | b- $C_1$ | 3.024 | 0.464 | 2.999 | 6.358 | 2.817 | 3.541 | 2.746 | 2.831 |
| | c- $C_1$ | 3.028 | 0.383 | 3.000 | 6.331 | 2.918 | 3.413 | 2.814 | 2.729 |
| | **d- $C_1$** | **3.092** | **0.630** | **1.000** | **6.388** | **2.838** | **3.550** | **2.799** | **2.888** |
| **17** | **a- $C_1$** | **3.099** | **0.485** | **2.999** | **6.250** | **2.770** | **3.480** | **2.755** | **2.823** |
| | b- $C_1$ | 3.033 | 0.375 | 3.004 | 6.210 | 2.834 | 3.376 | 2.808 | 2.801 |
| | c- $C_1$ | 3.078 | 0.560 | 2.999 | 6.371 | 2.791 | 3.580 | 2.775 | 2.822 |
| | d- $C_1$ | 3.043 | 0.537 | 2.999 | 6.227 | 2.718 | 3.509 | 2.755 | 2.867 |
| | e- $C_1$ | 3.085 | 0.630 | 2.999 | 6.193 | 2.599 | 3.594 | 2.747 | 2.876 |
| **18** | a- $C_{2v}$ | 3.056 | 0.478 | 2.999 | 6.492 | 3.053 | 3.439 | 2.786 | 2.795 |
| | b- $C_1$ | 3.104 | 0.543 | 3.000 | 6.349 | 2.914 | 3.435 | 2.776 | 2.875 |
| | c- $C_{6v}$ | 3.016 | 0.433 | 3.000 | 6.351 | 2.906 | 3.445 | 2.612 | 2.922 |
| | d- $C_s$ | 3.036 | 0.614 | 4.999 | 6.029 | 2.641 | 3.388 | 2.801 | 2.722 |
| | **e- $C_1$** | **3.107** | **0.682** | **2.999** | **6.413** | **2.728** | **3.685** | **2.723** | **3.041** |
| **19** | a- $C_s$ | 3.049 | 0.339 | 3.000 | 6.284 | 2.932 | 3.352 | 2.769 | 2.701 |
| | b- $C_1$ | 3.081 | 0.540 | 2.999 | 6.207 | 2.699 | 3.508 | 2.771 | 2.764 |
| | **c- $C_1$** | **3.116** | **0.552** | **2.995** | **6.293** | **3.092** | **3.201** | **2.714** | **2.836** |

| | | | | | | | | | |
|---|---|---|---|---|---|---|---|---|---|
| | d- $C_{6v}$ | 3.086 | 0.457 | 1.000 | 6.389 | 2.929 | 3.460 | 2.672 | 2.887 |
| | e- $C_{2v}$ | 3.068 | 0.263 | 2.999 | 5.899 | 2.626 | 3.273 | 2.747 | 2.874 |
| | f- $C_s$ | 3.115 | 0.453 | 4.993 | 5.963 | 2.670 | 3.293 | 2.745 | 2.923 |

## Figure captions

Fig. 01**:** Lowest energy structure and their corresponding isomers of $Ge_{n+1}$ (n=1-19) clusters. For each size, the lowest-energy isomers are reported in bold character.

Fig02. Lowest energy structure and their corresponding isomers of $VGe_n$ (n=1-19) clusters. For each size, the lowest-energy isomers are reported in bold character.

Fig. 03: Size dependence of the binding energy of $Ge_{n+1}$ and $VGe_n$ (n=1-19) clusters.

Fig. 04: Evolution of the HOMO-LUMO gaps of $Ge_{n+1}$ and $VGe_n$ (n=1-19) clusters as a function of cluster size.

Fig. 05: Size dependence of the second order energy difference of $Ge_{n+1}$ and $VGe_n$ (n=1-19) clusters.

Fig. 06: Size dependence of the vertical ionization potential (VIP) of $Ge_{n+1}$ and $VGe_n$ (n=1-19) clusters.

Fig. 07: Size dependence of the vertical electronic affinity of $Ge_{n+1}$ and $VGe_n$ (n=1-19) clusters.

Fig. 08: Size dependence of the chemical hardness of $Ge_{n+1}$ and $VGe_n$ (n=1-19) clusters.

Fig. 09: Size dependence of the total spin magnetic moment of $VGe_n$ (n=1-19) clusters.

Fig. 10: The projected density of states (PDOS) for $VGe_n$ (n=1-19) clusters.

Fig. 11**:** Density of states (DOS) of $VGe_{14}$ for alpha spin electrons. DOS for beta spin electrons are similar but the last three-fold degenerate orbital referred as 1G is empty (quartet state). For each band, the Kohn-Sham orbitals are plotted.

TOC Graphic

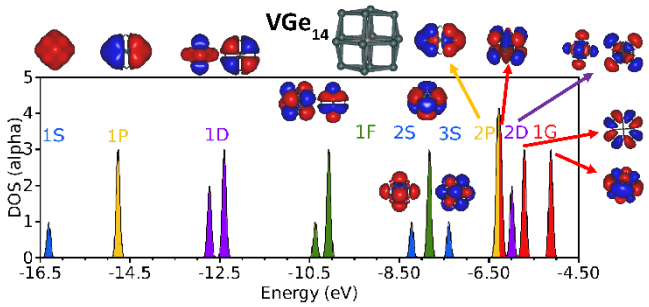
VGe14
1S
1P
1D
1F
2S
3S
2P
2D
1G
DOS (alpha)
Energy (eV)
-16.5
-14.5
-12.5
-10.5
-8.50
-6.50
-4.50

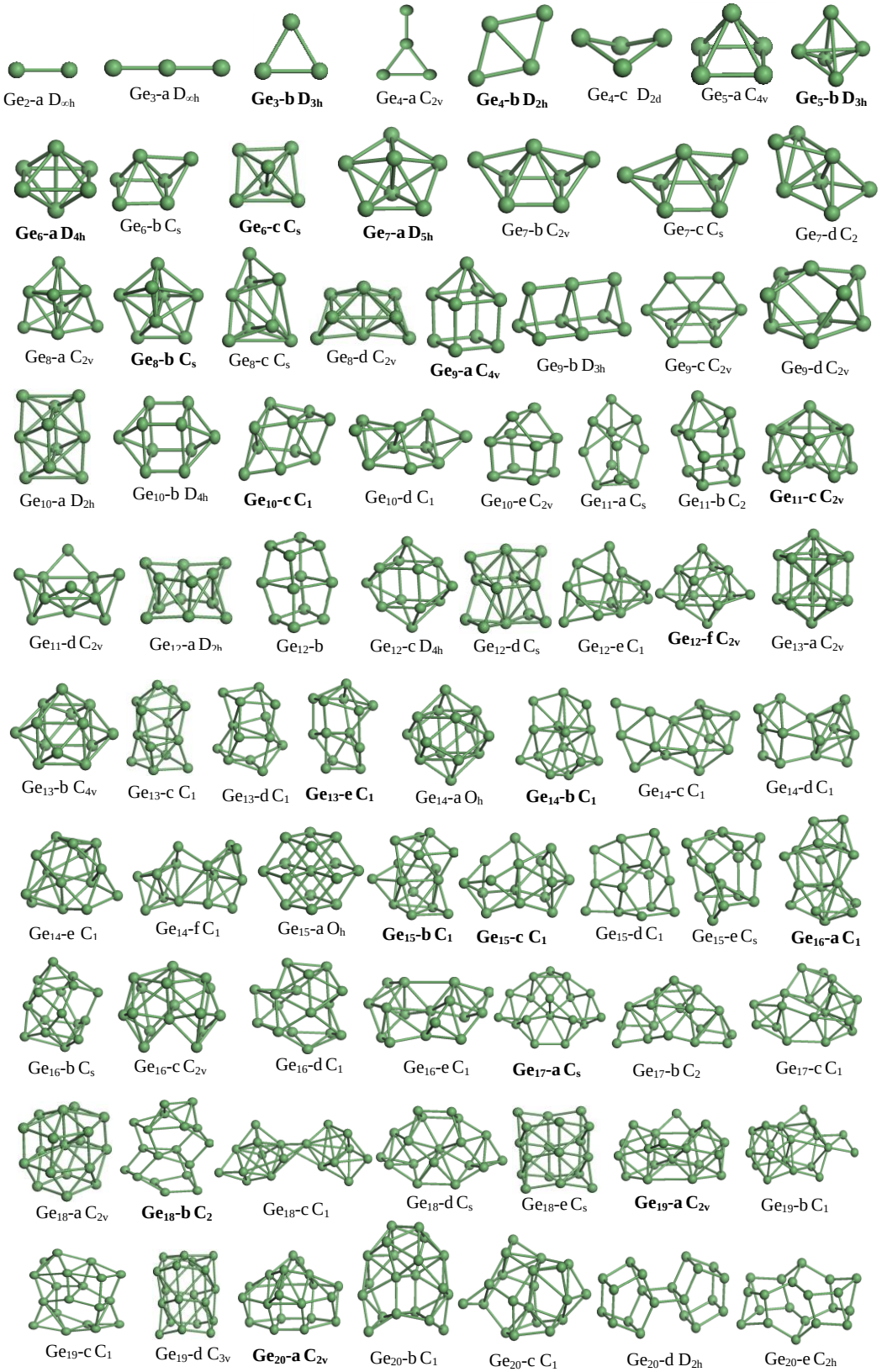


Fig. 01**:** Lowest energy structure and their corresponding isomers of $Ge_{n+1}$ (n=1-19) clusters. For each size, the lowest-energy isomers are reported in bold character.

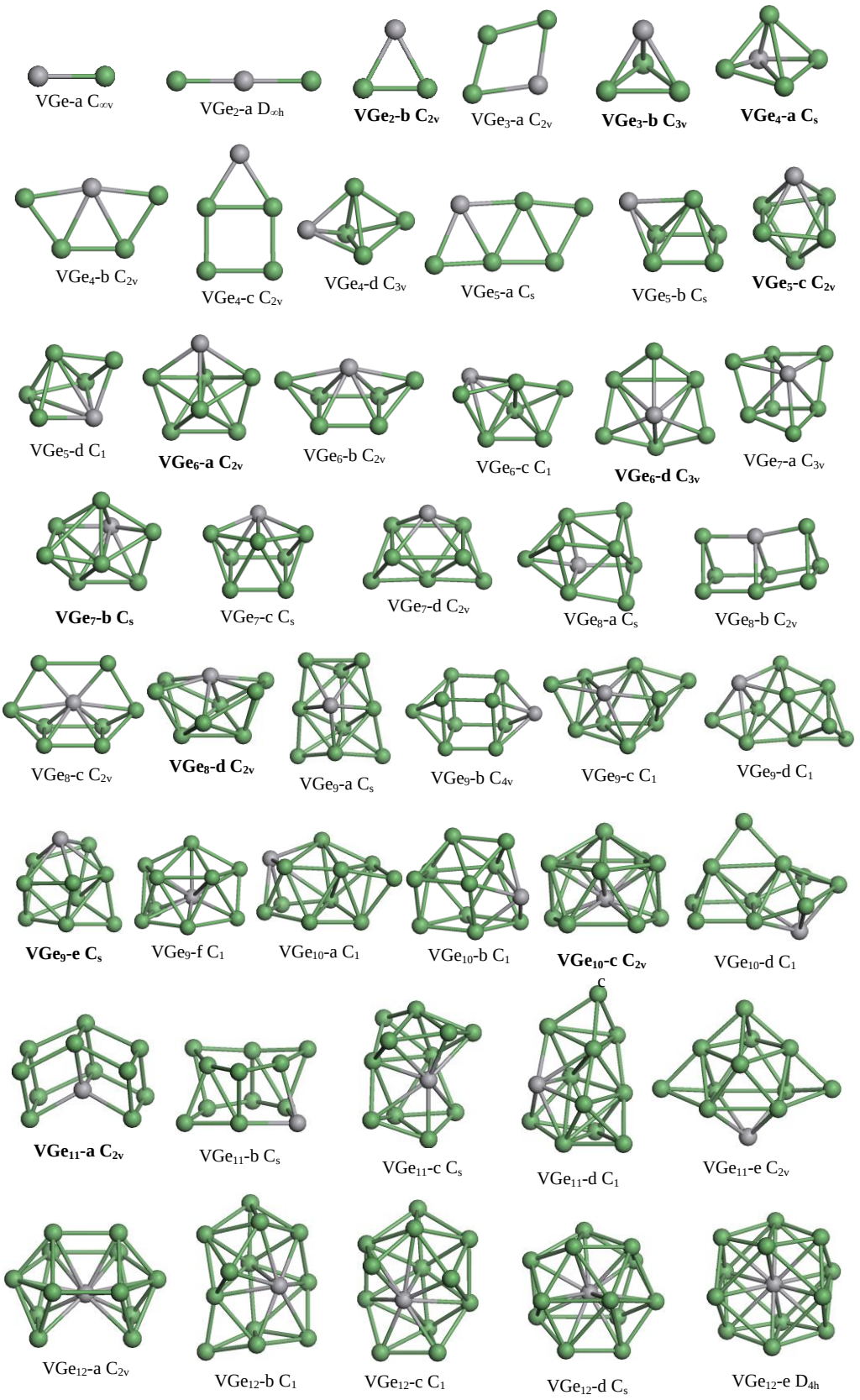


Fig02. Lowest energy structure and their corresponding isomers of $VGe_n$ (n=1-19) clusters. For each size, the lowest-energy isomers are reported in bold character.

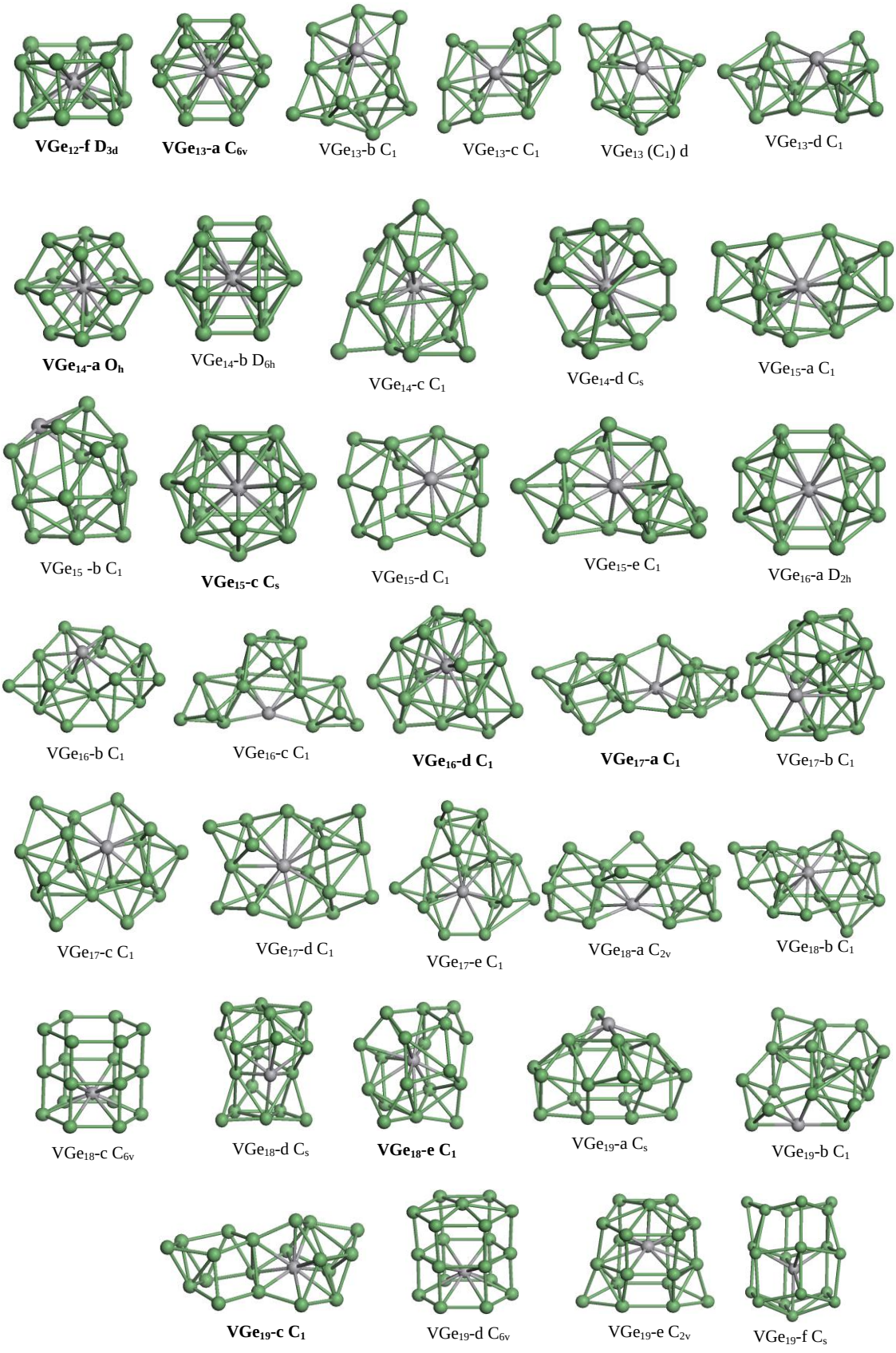


Fig02. Continued.

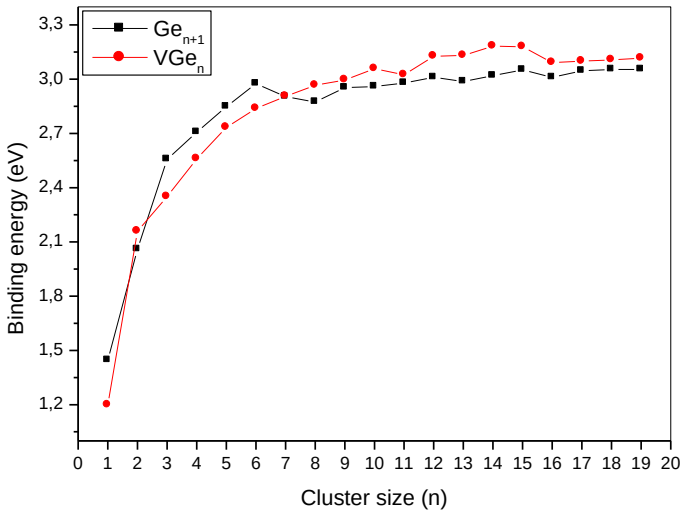


Fig. 03: Size dependence of the binding energy of $Ge_{n+1}$ and $VGe_n$ (n=1-19) clusters.

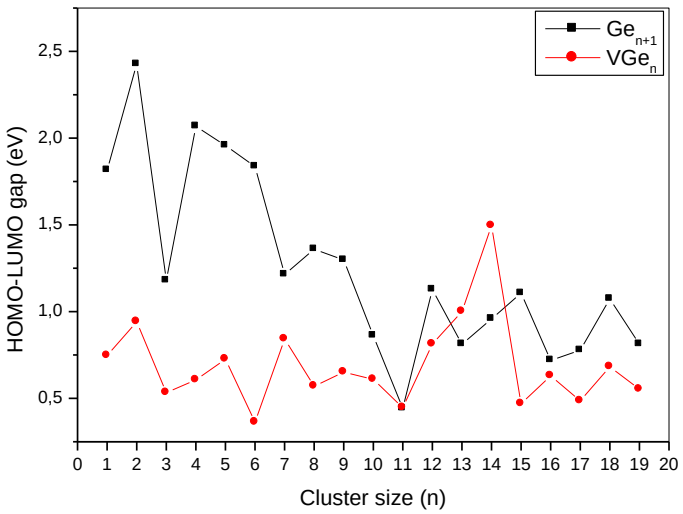


Fig. 04: Evolution of the HOMO-LUMO gaps of $Ge_{n+1}$ and $VGe_n$ (n=1-19) clusters as a function of cluster size.

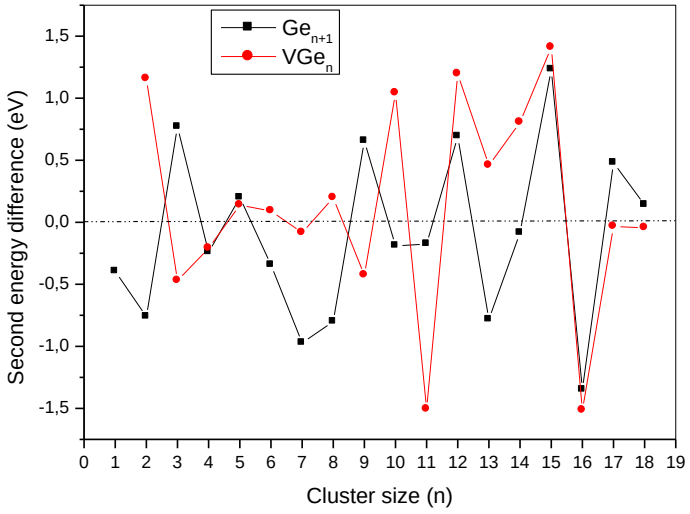


Fig. 05: Size dependence of the second order energy difference of $Ge_{n+1}$ and $VGe_n$ (n=1-19) clusters.

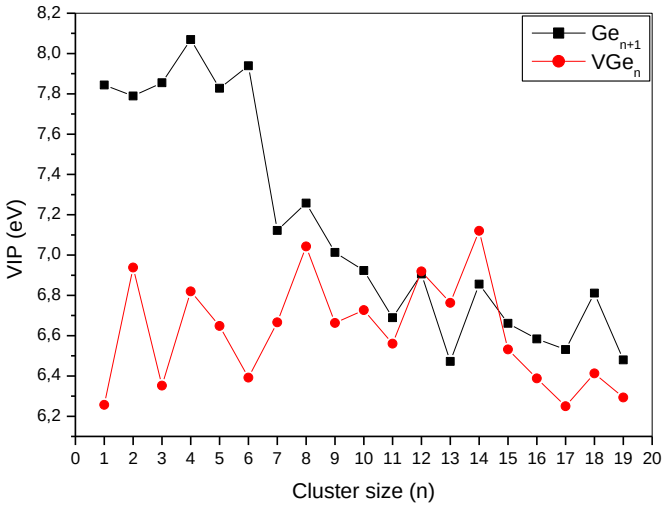


Fig. 06: Size dependence of the vertical ionization potential (VIP) of $Ge_{n+1}$ and $VGe_n$ (n=1-19) clusters.

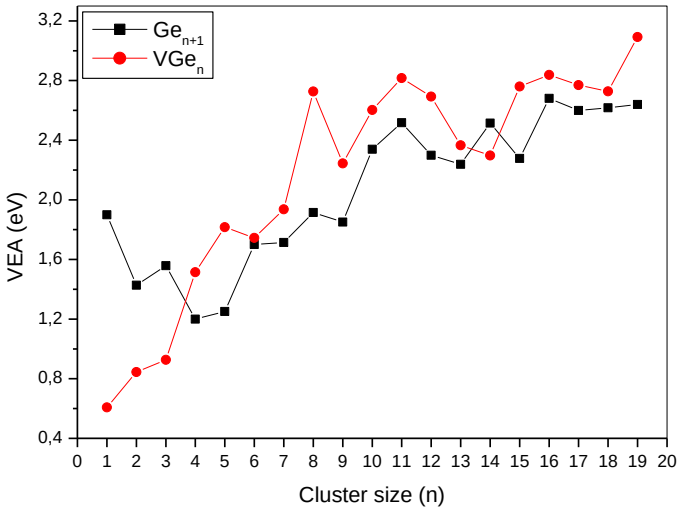


Fig. 07: Size dependence of the vertical electronic affinity of $Ge_{n+1}$ and $VGe_n$ (n=1-19) clusters.

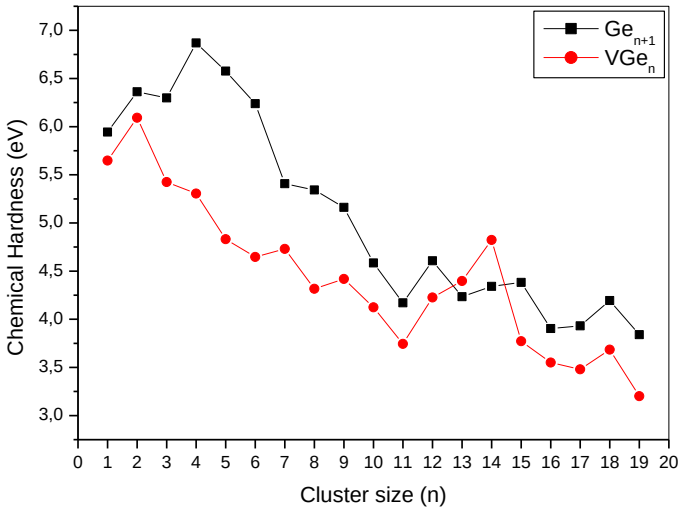


Fig. 08: Size dependence of the chemical hardness of $Ge_{n+1}$ and $VGe_n$ (n=1-19) clusters.

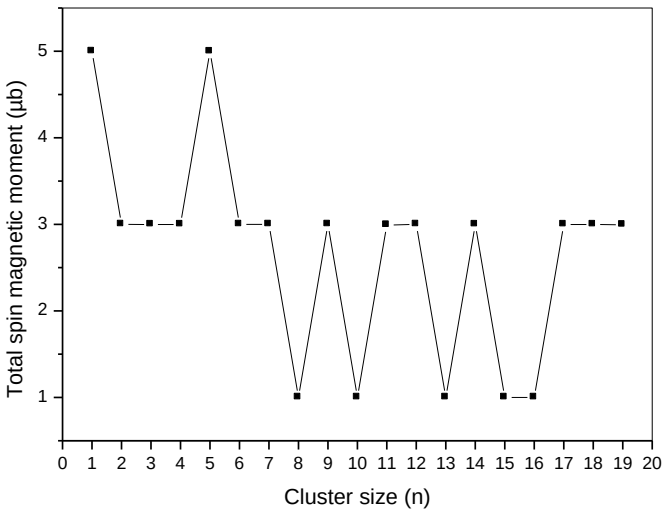


Fig. 09: Size dependence of the total spin magnetic moment of $VGe_n$ (n=1-19) clusters.

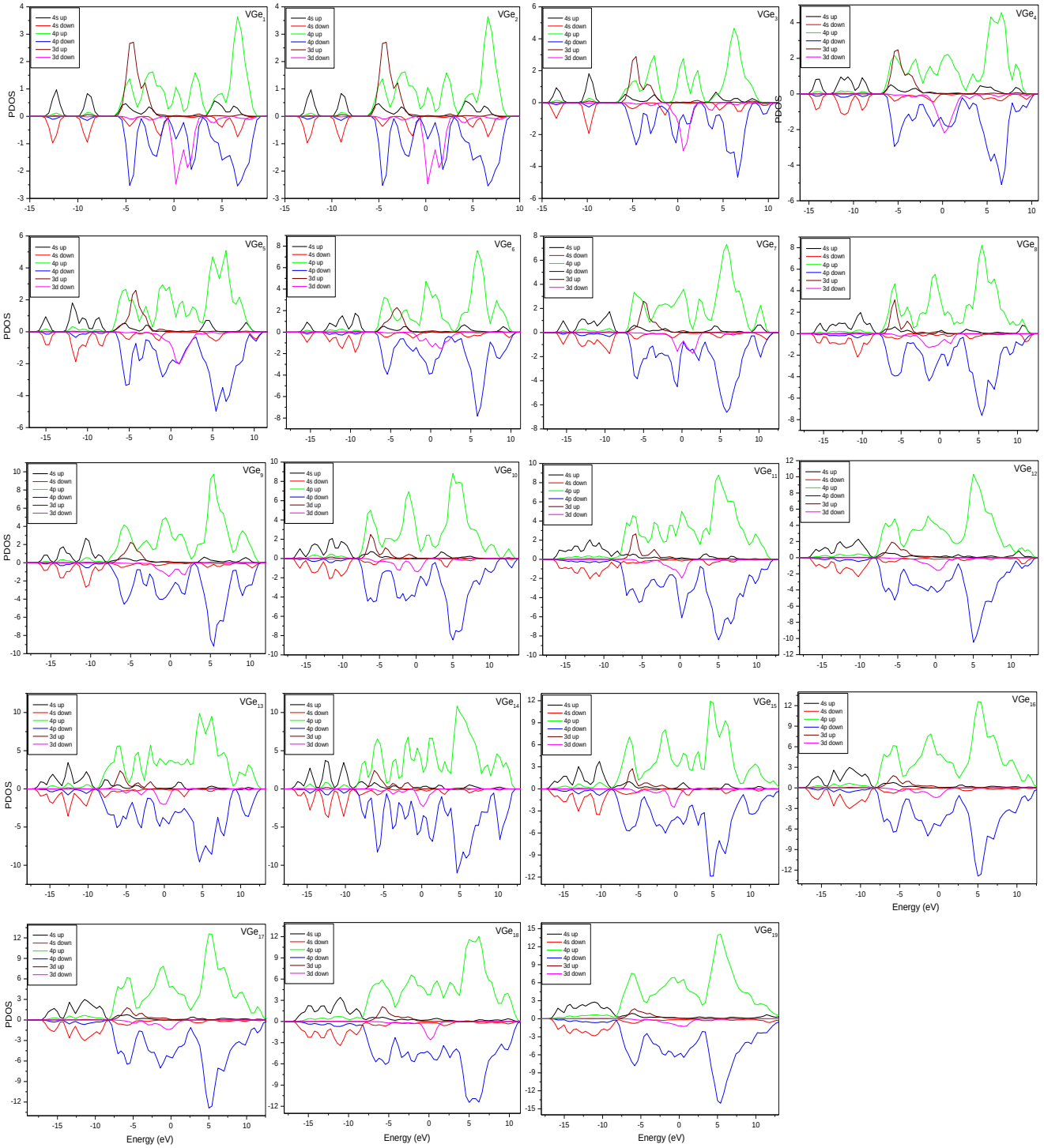


Fig. 10: The projected density of states (PDOS) for $VGe_n$ (n=1-19) clusters.

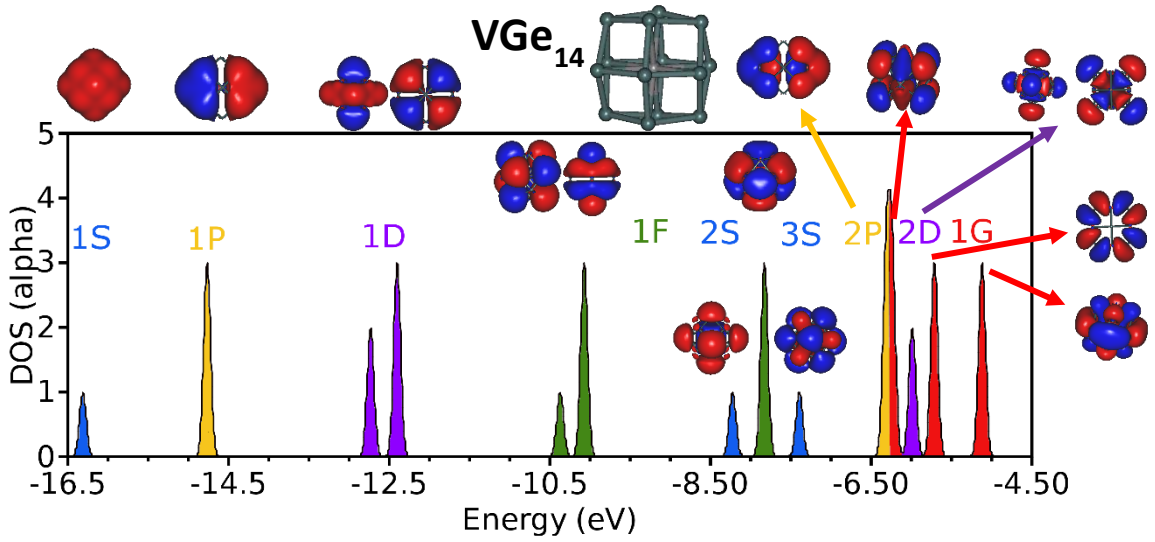


Fig. 11**:** Density of states (DOS) of $VGe_{14}$ for alpha spin electrons. DOS for beta spin electrons are similar but the last three-fold degenerate orbital referred as 1G is empty (quartet state). For each band, the Kohn-Sham orbitals are plotted.